

DEVELOPMENT OF A NON-LINEAR INJECTION KICKER FOR THE TPS STORAGE RING*

C. K. Yang[†], F. Y. Lin, H. Chen, H. H. Chen, Y. L. Chu

National Synchrotron Radiation Research Center, Hsinchu, Taiwan

Abstract

The TPS storage ring utilizes a standard four-kicker bump off-axis injection method. However, this approach is known to disrupt the stored beam during injections. The concept of a non-linear kicker (NIK) injection offers a potential solution to enable top-off injection while minimizing beam oscillation. This non-linear kicker features zero B_x and B_y fields at the center, with an off-axis B_y displacement of 15 mm for the TPS case. In this paper, we present the magnetic circuit design, considerations, fabrication process, and initial field measurement results of the TPS non-linear injection kicker.

INTRODUCTION

Top-up injection represents a standard mode for the stable operation of storage rings in most existing synchrotron radiation light source facilities. This operational mode requires frequent injection of electron beams into the storage ring. The Taiwan Photon Source (TPS) also employs this mode, utilizing four pulsed kicker magnets to create a closed local bump around the injection point. However, technical challenges such as pulse jitters, shapes, and field errors make it difficult for these four kicker pulsed kickers to perfectly match, resulting in oscillations of the stored beam and perturbing user experiments.

The concept of injecting electron beams into a storage ring using a single pulsed multipole magnet has been proposed and tested to address this issue [1, 2]. However, injection efficiencies may suffer when the injected beam size is too large, leading to an increase in the stored beam size due to multipole field components at the center. The ideal magnet field distribution requires near-zero dipole and quadrupole terms at the stored beam position while maximizing values at the position of the injected beam. BESSY [3] first proposed that such a magnetic field distribution could be created by a novel nonlinear kicker design featuring eight conductors deposited symmetrically in four quadrants of a transverse space. This nonlinear kicker magnet has been constructed as an in-vacuum type and successfully tested in the BESSY II storage ring. Subsequently, numerous facilities, including MAX IV [4], SOLEIL [5], Sirius [6], Diamond [7], and SLS-II [8], have adopted this NIK design to upgrade their injection scheme due to its transparent injection, compactness, and simplicity.

DESIGN CONSIDERATION

Requirements for the NIK

To enhance the TPS injection process, we have decided to test the non-linear kicker injection scheme without altering the current layout of the injection section. As depicted in Fig. 1, the NIK will be positioned between K3 and K4. The strengths of the dipoles (CH-4 and CH-5) and septum 2 are adjusted to alter the paths of the injected beam (shown as the red dashed line) before and after septum 2 to align with the NIK injection angle. The injection position in the transverse direction is 15 mm from the storage ring centerline, and the deflection angle is 3.2 mrad.

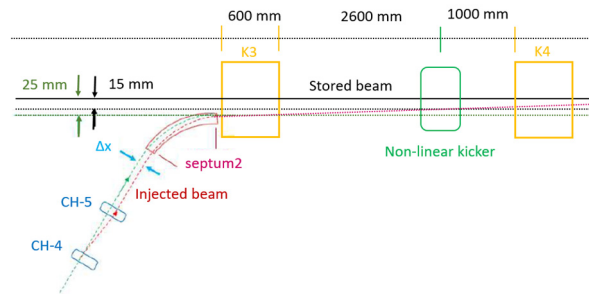


Figure 1: Layout of the TPS storage ring injection straight section.

Table 1: Main NIK Design Specifications

| Margin | Value |
|--|----------------------------------|
| Integrated field at the injected beam position | $3.2 \times 10^{-2} \text{ T m}$ |
| Total magnet length | 360 mm |
| Position of the peak magnetic field | 15 mm |
| Nominal NIK deflection angle | 3.2 mrad |
| Current pulse | half-sinusoidal |
| Pulse duration (μs) | 2 |

Since the electron beam energy is 3 GeV, the required integral field can be calculated to be 0.032 Tm. With the total length of NIK being 360 mm, the required field strength is calculated to be 888 G. However, injecting with a gradient field may lead to injection problems and a decrease in injection efficiency [6]. Therefore, it is essential that the injection position at the entrance of the NIK is at the peak magnetic field. Simultaneously, the field gradient in the central region of the NIK must be minimized to reduce the influence of the stored beam. The NIK is excited using a half-sinusoidal pulsed current with a duration of 2 μs. Table 1 summarizes the design requirements and parameters of the NIK.

* Work supported by the Ministry of Science and Technology, Taiwan, under contract with the Taiwan Photon Source.

† yang.ck@nsrrc.org.tw

Design of NIK

We conducted simulations of the NIK using OPERA 3D. The primary concept of the NIK is to generate a non-linear pulsed field with a maximum at the injected beam position and an extended zero plateau in the center. The model constructed in OPERA 3D is depicted in the inset of Fig. 2. The main structure of the NIK comprises eight conductors and a titanium-coated ceramic chamber, which serve as structural support and position the conductors. These copper wires are mounted on a ceramic tube with eight precisely machined grooves. These grooves are longitudinally machined on the ceramic tube to ensure accuracy. Additionally, the ceramic tube enables rapid changes in magnetic fields without significant distortion due to eddy currents.

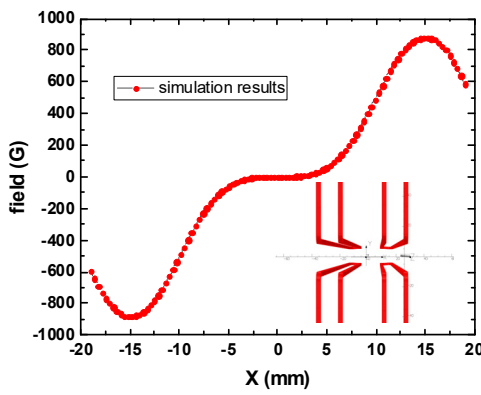


Figure 2: Opera model and simulation results.

The field-free region, as depicted in Fig. 2, is designed to be ± 1.5 mm around the stored beam center. The nominal peak field is set at 890 G at 15 mm. However, the nonlinear response of the yoke material may result in a non-zero field at the magnet center [9]. To mitigate this effect, we have opted not to use a yoke. However, achieving the required field strength without a yoke needs a very large current. Therefore, our NIK is designed to be an in-vacuum type to minimize the magnet gap. The total length of the NIK with the chamber is approximately 520 mm.

The simulation results indicate that the return conductor has an impact on the first integral field. Fig. 3a illustrates a symmetric return conductor design, where the transverse return conductor generates a vertical field. In a symmetric return conductor design, the vertical fields produced by the upper and lower conductors can cancel out due to the reverse current of the conductors. Consequently, a symmetric return conductor design results in a wider field region. On the other hand, in the case of a non-symmetric return conductor, as shown in Fig. 3b, the residual field generates a quadrupole field. Additionally, the position errors of the eight conductors degrade the field-free region.

The gap of the NIK is 8 mm, and the ceramic tube requires a thickness of 3 mm, constraining the minimal height of the inner conductor and the optimization of the field. The eight conductors are embedded in the grooves of

the ceramic tube. Positioning errors of these conductors introduce field errors in the field-free region. Therefore, the grooves should be machined with tolerances smaller than 20 μ m, and the top of each conductor is fixed by twenty ceramic plates to prevent detachment from the groove.

The required conductor current is 1570 A, with a rising time of 0.6 μ s and a calculated inductance of 1.8 μ H. Considering the addition of a 1 m cable between the power supply and the magnet wiring interconnects, the real inductance is expected to be higher than the calculated value. Due to this increased inductance and the short rising time, the required voltage of the power supply is estimated to be approximately 12 kV.

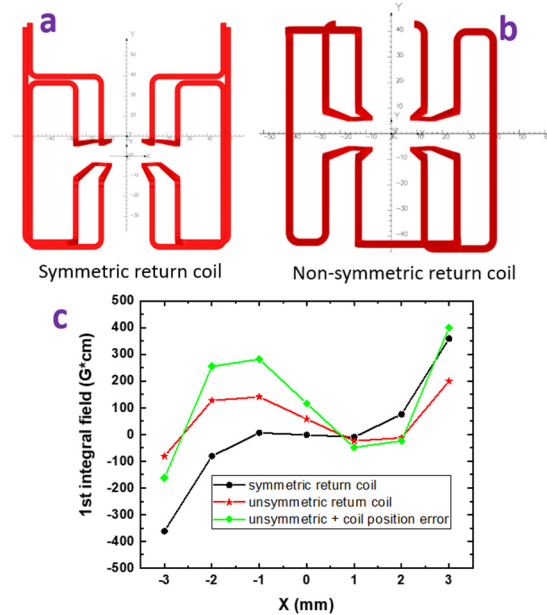


Figure 3: Symmetric and non-symmetric designs.

Table 2: Main NIK Design Parameters

| Margin | Value |
|-------------------------------------|--------------|
| Total length with chamber | 520 mm |
| Position of the peak magnetic field | 15 mm |
| Magnet aperture (hor. x ver.) | 42 mm x 8 mm |
| Nominal peak field | 890 G |
| Nominal peak excitation current | 1570 A |
| Nominal central magnetic field | < 0.2 G |
| Nominal voltage | 12 kV |
| Magnet inductance | 1.8 μ H |

The inductance of an NIK is an important parameter that allows the flow of the image current without disturbing the magnetic field. To address the inductance issue, a titanium layer will be coated on the inner surface of the ceramic tube. The thickness of this layer should be carefully chosen to balance the heat load caused by the beam-induced image currents and the attenuation of the field strength due to the induced eddy currents. It is planned to be 5 μ m to achieve this purpose. Table 2 lists the main design parameters of the NIK.

PROTOTYPE AND MEASUREMENT

A prototype consisting of only eight conductors and a ceramic tube has been constructed for initial study. The non-symmetric design was adopted due to its simplicity. The return conductors are positioned at least 100 mm away from the center to reduce residual fields. After assembling the NIK prototype, we measured the integral field distribution using a long search conductor specifically designed for detecting pulsed magnetic fields. The field measurement setup of the prototype is depicted in Fig. 4. It consists of a single turn and is constructed using printed circuit board (PCB) technology to ensure precise conductor positioning. The conductor dimensions are 700 mm in length and 0.3 mm in width. It is mounted on a stage equipped with two axes and a rotation axis.

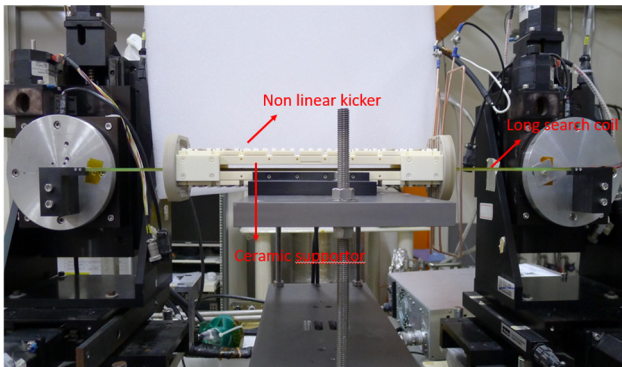


Figure 4: Field measurement setup.

The conductance of the NIK is measured using an LCR meter, with the result showing that the conductance of the NIK itself is about $1.9 \mu\text{H}$. However, the additional cables between the power supply and NIK significantly increase the conductance. The length and thickness of these cables are crucial factors. Shorter and thicker cables can reduce the conductance from $6.6 \mu\text{H}$ to $3.6 \mu\text{H}$. Nevertheless, a new configuration is required to minimize the conductance further.

A homemade power supply is utilized to deliver a $2 \mu\text{s}$ duration half-sine pulse voltage to the NIK. The pulsed current is measured by a standard PEARSON 101 current monitor, capable of measuring a peak current of 50000 A and featuring a rapid rising time of 100 ns. An oscilloscope is employed to measure the signals from both the current monitor and the induced electromotive force of the long search conductor. Trigger signals from a function generator are provided to synchronize the operations of the power supply, current monitor, and oscilloscope.

Figure 5 depicts the integral field measurement results. The peak field is located at $x = 15 \text{ mm}$ as expected, and the field strength is consistent with the simulation results. However, the zero-field zone in the central region of the magnet is slightly worse than the simulation result, and the two field peak strengths at $x = \pm 15 \text{ mm}$ are not identical. This discrepancy may be attributed to the position errors of the eight main conductors.

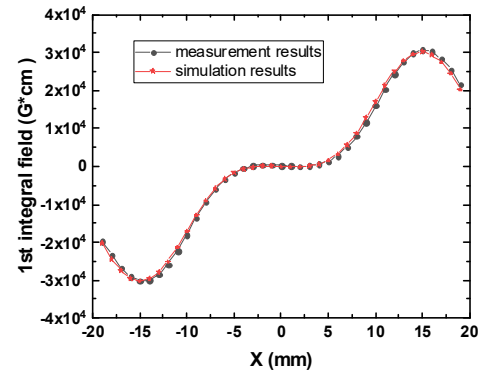


Figure 5: Field measurement results.

CONCLUSION

A nonlinear kicker for the TPS injection system has been designed and constructed. The preliminary field measurement results of the prototype show that the field strength at the kick point can be achieved, and the central region of the magnet does indeed have a zero-field zone, consistent with the simulation results. However, some correction conductors are being considered to compensate for the residual field produced by position errors in the eight main conductors.

REFERENCES

- [1] K. Harada, Y. Kobayashi, T. Miyajima, and S. Nagahashi, “New injection scheme using a pulsed quadrupole magnet in electron storage rings”, *Phys. Rev. ST Accel. Beams*, vol. 10, p. 123501, Dec. 2007.
doi:10.1103/PhysRevSTAB.10.123501
- [2] H. Takaki *et al.*, “Beam injection with a pulsed sextupole magnet in an electron storage ring”, *Phys. Rev. ST Accel. Beams*, vol. 13, p. 020705, Feb. 2020.
doi:10.1103/PhysRevSTAB.13.020705
- [3] T. Atkinson, M. Dirsat, O. Dressler, P. Kuske, and H. Rast, “Development of a Non-Linear Kicker System to Facilitate a New Injection Scheme for the BESSY II Storage Ring”, in *Proc. IPAC’11*, San Sebastian, Spain, Sep. 2011, paper THPO024, pp. 3394-3396.
- [4] S. C. Leemann, “Pulsed Multipole Injection for the MAX IV Storage Rings”, presented at Low Emittance Rings Workshop (LER2015), ESRF, Grenoble, France, Sep. 2015.
- [5] R. Ollier *et al.*, “Toward Transparent Injection with a Multipole Injection Kicker in a Storage Ring,” *Phys. Rev. Accel. Beams*, vol. 26, p. 020101, Feb. 2023.
doi:10.1103/PhysRevAccelBeams.26.020101
- [6] L. Liu, X. R. Resende, A. R. D. Rodrigues, and F. H. de Sá, “Injection Dynamics for Sirius Using a Nonlinear Kicker”, in *Proc. IPAC’16*, Busan, Korea, May 2016, pp. 3406-3408.
doi:10.18429/JACoW-IPAC2016-THPMR011
- [7] T. Pulampong and R. Bartolini, “A Non-linear Injection Kicker for Diamond Light Source”, in *Proc. IPAC’13*, Shanghai, China, May 2013, paper WEPWA065, pp. 2268-2270.

[8] B. MacDonald-de Neeve, M. Paraliev, and A. Saa Hernandez, “An Optimization Tool to Design a Coreless Non-Linear Injection Kicker Magnet”, in *Proc. IPAC'17*, Copenhagen, Denmark, May 2017, pp. 3170-3173.
doi:10.18429/JACoW-IPAC2017-WEPIK097

[9] S. C. Leemann, “Pulsed sextupole injection for Sweden’s new light source MAX-IV,” *Phys. Rev. Accel. Beams*, vol. 15, p. 050705, May 2012.
doi:10.1103/PhysRevSTAB.15.050705